AD-A148 141

(12)

AD

TECHNICAL REPORT ARLCB-TR-84029

BLAST COMPUTATION USING HARTEN'S TOTAL VARIATION DIMINISHING SCHEME

GARRY C. CAROFANO

DTIC
ELECTE
NOV 30 1984
S D
B

OCTOBER 1984

US ARMY ARMAMENT RESEARCH AND DEVELOPMENT CENTER
LARGE CALIBER WEAPON SYSTEMS LABORATORY
BENET WEAPONS LABORATORY
WATERVLIET N.Y. 12189

APPROVED FOR PUBLIC RELEASE; DISTRIBUTION UNLIMITED

DTIC FILE COPY

84 11 26 076

DISCLAIMER

The findings in this report are not to be construed as an official Department of the Army position unless so designated by other authorized documents.

The use of trade name(s) and/or manufacture(s) does not constitute an official indorsement or approval.

DISPOSITION

Destroy this report when it is no longer needed. Do not return it to the originator.

SECURITY CLASSIFICATION OF THIS PAGE *(When Data Entered)*

REPORT DOCUMENTATION PAGE

READ INSTRUCTIONS BEFORE COMPLETING FORM

1. REPORT NUMBER: ARLCB-TR-84029	2. GOVT ACCESSION NO.: AD-A148 141
3. RECIPIENT'S CATALOG NUMBER:	
4. TITLE *(and Subtitle)*: BLAST COMPUTATION USING HARTEN'S TOTAL VARIATION DIMINISHING SCHEME	5. TYPE OF REPORT & PERIOD COVERED: Final
	6. PERFORMING ORG. REPORT NUMBER:
7. AUTHOR(s): Garry C. Carofano	8. CONTRACT OR GRANT NUMBER(s):
9. PERFORMING ORGANIZATION NAME AND ADDRESS: US Army Armament Research & Development Center, Benet Weapons Laboratory, SMCAR-LCB-TL, Watervliet, NY 12189	10. PROGRAM ELEMENT, PROJECT, TASK AREA & WORK UNIT NUMBERS: AMCMS No. 6111.02.H600.011, PRON No. 1A425M541A1A
11. CONTROLLING OFFICE NAME AND ADDRESS: US Army Armament Research & Development Center, Large Caliber Weapon Systems Laboratory, Dover, NJ 07801	12. REPORT DATE: October 1984
	13. NUMBER OF PAGES: 30
14. MONITORING AGENCY NAME & ADDRESS*(if different from Controlling Office)*:	15. SECURITY CLASS. *(of this report)*: UNCLASSIFIED
	15a. DECLASSIFICATION/DOWNGRADING SCHEDULE:

16. DISTRIBUTION STATEMENT *(of this Report)*

Approved for public release; distribution unlimited.

17. DISTRIBUTION STATEMENT *(of the abstract entered in Block 20, if different from Report)*

18. SUPPLEMENTARY NOTES

19. KEY WORDS *(Continue on reverse side if necessary and identify by block number)*

Blast Computation
Numerical Methods

20. ABSTRACT *(Continue on reverse side if necessary and identify by block number)*

A model for blast flow field calculations involving two distinct gases is described. It is based upon the Euler equations and Harten's Total Variation Diminishing (TVD) scheme is used as the equation solver. The eigenvalues and eigenvectors are first derived for a general equation of state. Then a particular equation of state is presented for a mixture of two ideal gases. The model predictions show good agreement with experimental data for a shock diffraction around a corner.

DD FORM 1 JAN 73 1473 EDITION OF 1 NOV 65 IS OBSOLETE

UNCLASSIFIED

SECURITY CLASSIFICATION OF THIS PAGE *(When Data Entered)*

TABLE OF CONTENTS

TABLES

LIST OF ILLUSTRATIONS

DTIC ELECTE NOV 30 1984 B

Accession For
NTIS
DTIC
Unannounced
Justification
By
Distribution/
Availability Codes
Dist Special
A-1

INTRODUCTION

The rapid discharge of propellant gas from a weapon produces a strong shock wave which propagates into the environment. Several shocks, contact surfaces, and vortices form within the developing plume and separation occurs at the weapon exit plane (see Figure 1). Further, the physical properties of the plume gas are often sufficiently different from those of air that it is of interest to take this into account. This report describes a model for such a flow based upon the Euler equations for a mixture of two gases. Harten's Total Variation Diminishing (TVD) scheme (ref 1) is used as the equation solver. For verification, the classic problem of shock diffraction around a corner is computed and compared with the experimental data of Skews (refs 2,3). In Reference 4, the model is used to analyze the origin of secondary shock waves frequently observed in the blast signature of shoulder fired weapons.

THE EULER EQUATIONS

Written in conservation form, the Euler equations take the form

$$\frac{\partial U}{\partial \tau} + \frac{\partial F(U)}{\partial X} + \frac{\partial G(U)}{\partial Y} + W(U) = 0 \qquad (1)$$

---

[1]Harten, A., "High Resolution Schemes for Hyperbolic Conservation Laws," Journal of Computational Physics, Vol. 49, 1983, pp. 357-393.

[2]Skews, B. W., "The Shape of a Diffracting Shock Wave," Journal of Fluid Mechanics, Vol. 29, Part 2, 1967, pp. 297-304.

[3]Skews, B. W., "The Perturbed Region Behind a Diffracting Shock Wave," Journal of Fluid Mechanics, Vol. 29, Part 4, 1967, pp. 705-719.

[4]Carofano, G. C., "Secondary Waves From Nozzle Blast," U.S. ARDC Technical Report No. ARLCB-TR-84028, Benet Weapons Laboratory, Watervliet, NY, October 1984.

where

$$U = \begin{bmatrix} \rho \\ m \\ n \\ E \\ S \end{bmatrix}, \quad F(U) = \begin{bmatrix} m \\ m^2/\rho + P \\ mn/\rho \\ (E+P)m/\rho \\ Sm/\rho \end{bmatrix},$$

$$G(U) = \begin{bmatrix} n \\ mn/\rho \\ n^2/\rho + P \\ (E+P)n/\rho \\ Sn/\rho \end{bmatrix}, \quad W(U) = \frac{\varepsilon n}{Y} \begin{bmatrix} 1 \\ m/\rho \\ n/\rho \\ (E+P)/\rho \\ S/\rho \end{bmatrix}$$

In these equations, ρ is the mixture density; $m = \rho u$, $n = \rho v$, are the momentum components and u, v are the velocity components in the X- and Y-directions, respectively; P is the pressure; E is the total energy per volume and is related to the specific internal energy, e, of the mixture by the expression

$$e = \left(\frac{E}{\rho} - \frac{(m^2+n^2)}{2\rho^2}\right) \tag{2}$$

S is the mass concentration of gas species "a" - it has the same units as density; ε is zero for planar flow and unity for axisymmetric flow; X and Y are the axial and radial directions, respectively. All variables have been non-dimensionalized with respect to a reference state ρ_o, P_o, and length R. Thus, $\rho = \rho'/\rho_o$, $m = m'/(\rho_o P_o)^{1/2}$, $n = n'/(\rho_o P_o)^{1/2}$, $E = E'/P_o$, $P = P'/P_o$,

$S = S'/\rho_o$, $X = X'/R$, $Y = Y'/R$, and $\tau = \tau'(P_o/\rho_o)^{1/2}/R$ where the primed quantities are the dimensional counterparts of those defined above.

The pressure is related to the thermodynamic state variables ρ and e through the equation of state. Rather than carrying the details of this relationship through the algebra of determining the eigenvalues and eigenvectors of the Euler equations, the equation of state will be written in the general form

$$P = P(\rho,m,n,E,S) = \bar{P}(\rho,e,M_f) \tag{3}$$

where M_f is the mass fraction of species "a" defined as

$$M_f = S/\rho \tag{4}$$

The acoustic speed, c, is determined from the equation of state by

$$c^2 = \left(\frac{\partial \bar{P}}{\partial \rho}\right)_{s,M_f}$$

where s is the specific entropy. Using the following general relationship for partial derivatives

$$\left(\frac{\partial \bar{P}}{\partial \rho}\right)_{s,M_f} = \left(\frac{\partial \bar{P}}{\partial e}\right)_{\rho,M_f} \left(\frac{\partial e}{\partial \rho}\right)_{s,M_f} + \left(\frac{\partial \bar{P}}{\partial \rho}\right)_{e,M_f}$$

and the thermodynamic identity (ref 5)

$$\bar{P} = \rho^2 \left(\frac{\partial e}{\partial \rho}\right)_{s,M_f}$$

the acoustic speed becomes

$$c^2 = \frac{\bar{P}}{\rho^2}\left(\frac{\partial \bar{P}}{\partial e}\right)_{\rho,M_f} + \left(\frac{\partial \bar{P}}{\partial \rho}\right)_{e,M_f} \tag{5}$$

---

[5]Obert, E. F., Concepts of Thermodynamics, McGraw-Hill Book Co. Inc., New York, 1960, Equation 11-1b.

The subscript "M_f" is used to indicate that the partial derivatives are evaluated for a specific mixture.

In what follows, other partial derivatives of pressure appear and some useful relationships exist among them. From Eq. (3),

$$P_\rho = \left(\frac{\partial P}{\partial \rho}\right)_{m,n,E,S} = \left(\frac{\partial P}{\partial \rho}\right)_{e,M_f} + \left(\frac{\partial P}{\partial e}\right)_{\rho,M_f} \left(\frac{\partial e}{\partial \rho}\right)_{m,n,E} + \left(\frac{\partial P}{\partial M_f}\right)_{\rho,e} \left(\frac{\partial M_f}{\partial \rho}\right)_{S} \tag{6a}$$

$$P_m = \left(\frac{\partial P}{\partial m}\right)_{\rho,n,E,S} = \left(\frac{\partial P}{\partial e}\right)_{\rho,M_f} \left(\frac{\partial e}{\partial m}\right)_{\rho,n,E,S} \tag{6b}$$

$$P_n = \left(\frac{\partial P}{\partial n}\right)_{\rho,m,E,S} = \left(\frac{\partial P}{\partial e}\right)_{\rho,M_f} \left(\frac{\partial e}{\partial n}\right)_{\rho,m,n,S} \tag{6c}$$

$$P_E = \left(\frac{\partial P}{\partial E}\right)_{\rho,m,n,S} = \left(\frac{\partial P}{\partial e}\right)_{\rho,M_f} \left(\frac{\partial e}{\partial E}\right)_{\rho,m,n,S} \tag{6d}$$

$$P_S = \left(\frac{\partial P}{\partial S}\right)_{\rho,m,n,E} = \left(\frac{\partial P}{\partial M_f}\right)_{\rho,e} \left(\frac{\partial M_f}{\partial S}\right)_{\rho} \tag{6e}$$

Equations (2) through (6) can be combined to give

$$P_m + u\, P_E = 0 \tag{7}$$

$$P_n + v\, P_E = 0 \tag{8}$$

$$c^2 = P_\rho + M_f P_S + (H - u^2 - v^2) P_E \tag{9}$$

where H is the total enthalpy per unit mass, defined as

$$H = \frac{E + P}{\rho} \tag{10}$$

The matrix manipulations required to determine the eigenvalues and eigenvectors are straightforward and will not be presented here. Suffice it to say that the combinations of variables and derivatives in Eqs. (7) through (10) appear frequently and lead to the compact and recognizable forms given

below*.

Let A denote the Jacobian matrix $\partial F(U)/\partial U$, or

$$A = \begin{bmatrix} 0 & 1 & 0 & 0 & 0 \\ -u^2 + P_\rho & 2u + P_m & P_n & P_E & P_S \\ -uv & v & u & 0 & 0 \\ -uH + uP_\rho & H + uP_m & vP_n & u(1+P_E) & uP_S \\ -uM_f & M_f & 0 & 0 & u \end{bmatrix} \tag{11}$$

Setting the determinant $|A-a_X I|$ equal to zero, where I is the identity matrix, and solving for the vector a_X of eigenvalues gives

$$(a_X^1, a_X^2, a_X^3, a_X^4, a_X^5) = (u-c, u, u, u+c, u) \tag{12}$$

*The author began this study based on a report written in early 1982 by Harten at the Courant Institute, New York University. That report, dealing mostly with theory, eventually appeared as Reference 1 in 1983. Subsequently, two more reports were written by Yee, Warming, and Harten (refs 6,7) which emphasized applications of the theory. Thus, as an aid to the reader, the present report will conform to the notation of the later works where convenient, but some of the symbols, indices, and even the "arrangement" of the arrays follow the preliminary work performed by the author in developing his computer program.

[1]Harten, A., "High Resolution Schemes for Hyperbolic Conservation Laws," Journal of Computational Physics, Vol. 49, 1983, pp. 357-393.

[6]Yee, H. C., Warming, R. F., and Harten, A., "A High-Resolution Numerical Technique For Inviscid Gas-Dynamic Problems With Weak Shocks," Preprint for Proceedings of the Eighth International Conference on Numerical Methods in Fluid Dynamics, Aachen, West Germany, June 1982.

[7]Yee, H. C., Warming, R. F., and Harten, A., "Implicit Total Variation Diminishing (TVD) Schemes for Steady-State Calculations," NASA Technical Memorandum 84342, March 1983.

The right-eigenvectors $R_X = (R_X^1, R_X^2, R_X^3, R_X^4, R_X^5)$ are

$$R_X = \begin{bmatrix} 1 & 1 & 0 & 1 & 0 \\ u-c & u & 0 & u+c & 0 \\ v & v & 1 & v & 0 \\ H-uc & H-c^2/P_E & v & H+uc & \Gamma \\ M_f & M_f & 0 & M_f & 1 \end{bmatrix} \tag{13}$$

and the left-eigenvectors $L_X = (L_X^1, L_X^2, L_X^3, L_X^4, L_X^5)$ are

$$L_X = \begin{bmatrix} (u/c + r)/2 & -(1/c + uq)/2 & -vq/2 & q/2 & -\Gamma q/2 \\ 1-r & uq & vq & -q & \Gamma q \\ -v & 0 & 1 & 0 & 0 \\ (-u/c + r)/2 & (1/c - uq)/2 & -vq/2 & q/2 & -\Gamma q/2 \\ -M_f & 0 & 0 & 0 & 1 \end{bmatrix} \tag{14}$$

where

$$\Gamma = -P_S/P_E \tag{15}$$

and

$$q = P_E/c^2 \quad , \quad r = P_\rho/c^2 = 1-q(H-u^2-v^2-M_f\Gamma) \tag{16}$$

Similarly, the Jacobian matrix $B = \partial G(U)/\partial U$ is

$$B = \begin{bmatrix} 0 & 0 & 1 & 0 & 0 \\ -uv & v & u & 0 & 0 \\ -v^2+P_\rho & P_m & 2v+P_n & P_E & P_S \\ -vH+vP_\rho & vP_m & H + vP_n & v(1+P_E) & vP_S \\ -vM_f & 0 & M_f & 0 & v \end{bmatrix} \tag{17}$$

with eigenvalues a_Y given by

$$(a_Y^1, a_Y^2, a_Y^3, a_Y^4, a_Y^5) = (v-c,\ v,\ v,\ v+c,\ v) \tag{18}$$

The right-eigenvectors $R_Y = (R_Y^1, R_Y^2, R_Y^3, R_Y^4, R_Y^5)$ are

$$R_Y = \begin{bmatrix} 1 & 1 & 0 & 1 & 0 \\ u & u & 1 & u & 0 \\ v-c & v & 0 & v+c & 0 \\ H-vc & H-c^2/P_E & u & H+vc & \Gamma \\ M_f & M_f & 0 & M_f & 1 \end{bmatrix} \tag{19}$$

and the left-eigenvectors $L_Y = (L_Y^1, L_Y^2, L_Y^3, L_Y^4, L_Y^5)$ are

$$L_Y = \begin{bmatrix} (v/c + r)/2 & -uq/2 & -(1/c + vq)/2 & q/2 & -\Gamma q/2 \\ 1-r & uq & vq & -q & \Gamma q \\ -u & 1 & 0 & 0 & 0 \\ (-v/c + r)/2 & -uq/2 & (1/c - vq)/2 & q/2 & -\Gamma q/2 \\ -M_f & 0 & 0 & 0 & 1 \end{bmatrix} \tag{20}$$

THE ALGORITHM

Operator splitting was used to solve Eq. (1) on a uniform grid. Harten's TVD scheme (refs 1,6,7) was applied to the two flux terms and Euler's predictor-corrector method was used to handle the source term. The solution at time τ, $U^n_{i,j}$, was advanced to time $\tau + 2\Delta\tau$ using the following sequence of operations:

$$U^{n+2}_{i,j} = L_X\, L_Y\, L_S\, L_S\, L_Y\, L_X\, U^n_{i,j} \tag{21}$$

where

$$L_X: \quad U^{*}_{i,j} = U^{n}_{i,j} - \frac{\Delta\tau}{\Delta X}\left(\hat{F}^{n}_{i+1/2,j} - \hat{F}^{n}_{i-1/2,j}\right) \tag{22a}$$

$$L_Y: \quad U^{**}_{i,j} = U^{*}_{i,j} - \frac{\Delta\tau}{\Delta Y}\left(\hat{G}^{*}_{i,j+1/2} - \hat{G}^{*}_{i,j-1/2}\right) \tag{22b}$$

$$L_S: \quad \begin{aligned} \bar{U}_{i,j} &= U^{**}_{i,j} - \Delta\tau\, W(U^{**}_{i,j}) \\ U^{n+1}_{i,j} &= [U^{**}_{i,j} + \bar{U}_{i,j} - \Delta\tau\, W(\bar{U}_{i,j})]/2 \end{aligned} \tag{22c}$$

The flux $\hat{F}_{i+1/2,j}$ is given by

$$\hat{F}_{i+1/2,j} = [F(U_{i,j}) + F(U_{i+1,j}) + (\Delta X/\Delta\tau) \sum_{k=1}^{5} \beta^k_{i+1/2,j}\, R^k_{i+1/2,j}]/2 \tag{23a}$$

$$\beta^k_{i+1/2,j} = (g^k_{i,j} + g^k_{i+1,j}) - Q(\nu^k_{i+1/2,j} + \gamma^k_{i+1/2,j})\,\alpha^k_{i+1/2,j} \tag{23b}$$

---

[1] Harten, A., "High Resolution Schemes for Hyperbolic Conservation Laws," Journal of Computational Physics, Vol. 49, 1983, pp. 357-393.

[6] Yee, H. C., Warming, R. F., and Harten, A., "A High-Resolution Numerical Technique For Inviscid Gas-Dynamic Problems With Weak Shocks," Preprint for Proceedings of the Eighth International Conference on Numerical Methods in Fluid Dynamics, Aachen, West Germany, June 1982.

[7] Yee, H. C., Warming, R. F., and Harten, A., "Implicit Total Variation Diminishing (TVD) Schemes for Steady-State Calculations," NASA Technical Memorandum 84342, March 1983.

$$g^k_{i,j} = s^k_{i+1/2,j} \max[0, \min(|\alpha^k_{i+1/2,j}|, \alpha^k_{i-1/2,j} s^k_{i+1/2,j}]/8 \quad (23c)$$

$$s^k_{i+1/2,j} = \text{sign}(\alpha^k_{i+1/2,j}) \quad (23d)$$

$$\gamma^k_{i+1/2,j} = \begin{cases} (g^k_{i+1,j} - g^k_{i,j})/\alpha^k_{i+1/2,j}, & \alpha^k_{i+1/2,j} \neq 0 \\ 0, & \alpha^k_{i+1/2,j} = 0 \end{cases} \quad (23e)$$

$$\nu^k_{i+1/2,j} = (\Delta\tau/\Delta X)\, a^k_{i+1/2,j} \quad (23f)$$

$$Q(z) = z^2 + 1/4 \quad (23g)$$

where $a^k_{i+1/2,j}$ and $R^k_{i+1/2,j}$ are given in Eqs. (12) and (13), respectively. The subscript i+1/2 signifies that all of the values in the functions are to be evaluated at some average state $(U_{i,j}, U_{i+1,j})$. In this study, this state was taken to be

$$\hat{u} = (u_{i,j} + u_{i+1,j})/2 \quad (24a)$$

$$\hat{v} = (v_{i,j} + v_{i+1,j})/2 \quad (24b)$$

$$\hat{c} = (c_{i,j} + c_{i+1,j})/2 \quad (24c)$$

$$\hat{H} = (H_{i,j} + H_{i+1,j})/2 \quad (24d)$$

$$\hat{M}_f = (M_{fi,j} + M_{fi+1,j})/2 \quad (24e)$$

$$\hat{P}_E = (P_{Ei,j} + P_{Ei+1,j})/2 \quad (24f)$$

$$\hat{\Gamma} = (\Gamma_{i,j} + \Gamma_{i+1,j})/2 \quad (24g)$$

The vector $\alpha^k_{i+1/2,j}$ is computed as follows:

$$\delta\rho = \rho_{i+1,j} - \rho_{i,j} \quad (25a)$$

$$\delta m = m_{i+1,j} - m_{i,j} \quad (25b)$$

$$\delta n = n_{i+1,j} - n_{i,j} \quad (25c)$$

$$\delta E = E_{i+1,j} - E_{i,j} \tag{25d}$$

$$\delta S = S_{i+1,j} - S_{i,j} \tag{25e}$$

$$C_1 = \hat{r}\delta\rho + \hat{q}(\delta E - \hat{u}\delta m - \hat{v}\delta n - \hat{\Gamma}\delta S) \tag{26a}$$

$$C_2 = (\delta m - \hat{u}\delta\rho)/\hat{c} \tag{26b}$$

$$\alpha^1_{i+1/2,j} = (C_1 - C_2)/2 \tag{26c}$$

$$\alpha^2_{i+1/2,j} = \delta\rho - C_1 \tag{26d}$$

$$\alpha^3_{i+1/2,j} = \delta n - \hat{v}\delta\rho \tag{26e}$$

$$\alpha^4_{i+1/2,j} = (C_1 + C_2)/2 \tag{26f}$$

$$\alpha^5_{i+1/2,j} = \delta S - \hat{M}_f\delta\rho \tag{26g}$$

The flux $\hat{G}_{i,j+1/2}$ is given by expressions similar to Eqs. (23), only with the subscript j varying; $a^k_{i,j+1/2}$ and $R^k_{i,j+1/2}$ are given by Eqs. (18) and (19), respectively. The vector $\alpha^k_{i,j+1/2}$ uses the analogues of Eqs. (24) and (25) with j varying. Finally

$$C_1 = \hat{r}\delta\rho + \hat{q}(\delta E - \hat{u}\delta m - \hat{v}\delta n - \hat{\Gamma}\delta S) \tag{27a}$$

$$C_2 = (\delta n - \hat{v}\delta\rho)/\hat{c} \tag{27b}$$

$$\alpha^1_{i,j+1/2} = (C_1 - C_2)/2 \tag{27c}$$

$$\alpha^2_{i,j+1/2} = \delta\rho - C_1 \tag{27d}$$

$$\alpha^3_{i,j+1/2} = \delta m - \hat{u}\delta\rho \tag{27e}$$

$$\alpha^4_{i,j+1/2} = (C_1 + C_2)/2 \tag{27f}$$

$$\alpha^5_{i,j+1/2} = \delta S - \hat{M}_f\delta\rho \tag{27g}$$

The time step, $\Delta\tau$, was calculated from the expression

$$\Delta\tau = \frac{0.85\ \Delta X}{\max_{i,j}[\max(|u_{i,j}|,|v_{i,j}|) + c_{i,j}]} \quad \text{all } i,j.$$

The CFL factor of 0.85 was suggested in Reference 1.

For axisymmetric calculations ($\varepsilon = 1$), the coefficient (n/Y) in the vector W(u), Eq. (1), becomes indeterminant on the axis because the radial component of momentum and Y both vanish. To overcome this difficulty, L'Hospital's rule is applied to Eq. (1). Since all of the terms are well behaved at Y = 0 except the coefficient (n/Y), only this factor is changed in the limiting process. It becomes

$$\frac{\partial n/\partial Y}{1} = \frac{\partial n}{\partial Y}$$

The following second order accurate Lagrange differentiation formula is used:

$$\frac{\partial n_o}{\partial Y} = \frac{1}{2\Delta Y}(-n_{-1} + n_1)$$

where the n_{-1}, n_o, and n_1 are the three points at j = -1, 0, and 1, respectively. By symmetry $n_{-1} = -n_1$, therefore,

$$\frac{\partial n_o}{\partial Y} = \frac{n_1}{\Delta Y}$$

COMMENT: The reader familiar with Harten's scheme will recognize that the "artificial compression" terms have been omitted from the flux expression in Eq. (23). These terms were found to be quite useful for "squaring the corners" at shocks and contact surfaces but frequently caused an entropy violation in regions where a shock was followed by an expansion or where an expansion was terminated by a shock. Reducing the amount of artificial

---

[1]Harten, A., "High Resolution Schemes for Hyperbolic Conservation Laws," Journal of Computational Physics, Vol. 49, 1983, pp. 357-393.

compression, as suggested in Reference 7, would alleviate the problem in one circumstance only to have it reappear in another. Because such regions are common to the problems of interest, the decision was made, quite reluctantly, to omit the compression terms over the entire flow field.

Secondly, the reader will note that the "average state" defined above differs from the two choices suggested in References 1, 6, and 7. One choice, Roe's method, uses a "mean value Jacobian" such that

$$F(U_{i+1,j}) - F(U_{i,j}) = \hat{A}(U_{i,j},U_{i+1,j})(U_{i+1,j} - U_{i,j})$$

For an ideal gas it is not difficult to calculate the proper $\hat{u}$, $\hat{v}$,... from this expression, but for more general equations of state the required result is difficult to obtain.

The second choice, $(U_{i,j} + U_{i+1,j})/2$, occasionally produced poor results when used with more general equations of state. It first averages the conserved variables, then calculates the required quantities, $\hat{u}$, $\hat{v}$, $\hat{c}$,... from the average state.

The method used here, Eq. (24), evaluates the variables at each location, then forms the required average. This worked consistently well for various state equations; for an ideal gas, it produced essentially the same solutions as were obtained with Roe's averaging.

---

[1]Harten, A., "High Resolution Schemes for Hyperbolic Conservation Laws," Journal of Computational Physics, Vol. 49, 1983, pp. 357-393.

[6]Yee, H. C., Warming, R. F., and Harten, A., "A High-Resolution Numerical Technique For Inviscid Gas-Dynamic Problems With Weak Shocks," Preprint for Proceedings of the Eighth International Conference on Numerical Methods in Fluid Dynamics, Aachen, West Germany, June 1982.

[7]Yee, H. C., Warming, R. F., and Harten, A., "Implicit Total Variation Diminishing (TVD) Schemes for Steady-State Calculations," NASA Technical Memorandum 84342, March 1983.

THE STATE EQUATION

The present model was developed as an aid for interpreting some experimental results obtained with a blast simulator (ref 4). Mixing of the helium driver gas with air occurs in the system and an equation of state for the mixture is needed.

The state variables in the Euler equations are the density, ρ, and the specific internal energy, e. The latter has units of energy per unit mass, but the properties of a mixture of gases are best determined on a molal basis (ref 8). Molal units will therefore be used in the intermediate steps leading to the desired function $P = \bar{P}(\rho,e,M_f)$.

Consider a mixture of two ideal gases containing mass m_a of species "a" and mass m_b of species "b". The mass fraction, M_f, of species "a" is then

$$M_f = \frac{m_a}{m_a + m_b}$$

The number of moles, n, of each species is

$$n_a = \frac{m_a}{M_a} \quad , \quad n_b = \frac{m_b}{M_b}$$

where M_a, M_b, are the respective molecular weights. The mole fractions are

$$x_a = \frac{n_a}{n_a + n_b} \quad , \quad x_b = \frac{n_b}{n_a + n_b}$$

For the mixture

$$M = x_a M_a + x_b M_b$$

---

[4]Carofano, G. C., "Secondary Waves From Nozzle Blast," U.S. ARDC Technical Report No. ARLCB-TR-84028, Benet Weapons Laboratory, Watervliet, NY, October 1984.

[8]Obert, E. F., Concepts of Thermodynamics, McGraw-Hill Book Co. Inc., New York, 1960, Chapter 8.

$$c_v = x_a c_{va} + x_b c_{vb}$$

$$c_p = x_a c_{pa} + x_b c_{pb}$$

where c_v and c_p are the molal specific heats at constant volume and constant pressure, respectively. For each gas

$$c_{va} = \frac{R_o}{\gamma_a - 1} \quad , \quad c_{vb} = \frac{R_o}{\gamma_b - 1}$$

where R_o is the universal gas constant in molal units. The specific internal energy of the mixture is

$$e = \frac{(x_a c_{va} + x_b c_{vb})T}{M}$$

where T is the temperature; the reference state is taken as absolute zero. The state equation for the mixture is

$$\bar{P} = \frac{\rho R_o T}{M}$$

or, using the above definitions,

$$\bar{P} = \frac{\rho e}{\left(\frac{x_a}{\gamma_a - 1} + \frac{x_b}{\gamma_b - 1}\right)} \tag{28}$$

The specific heat ratio for the mixture is defined as

$$\gamma = c_p / c_v$$

With a little algebra the following results are obtained:

$$\frac{1}{\gamma - 1} = \frac{x_a}{\gamma_a - 1} + \frac{x_b}{\gamma_b - 1} \tag{29}$$

$$\gamma = \frac{M_f(\gamma_a - \sigma\gamma_b) + \sigma\gamma_b}{M_f(1-\sigma) + \sigma} \tag{30}$$

$$\gamma_{M_f} = \frac{\partial \gamma}{\partial M_f} = \frac{\sigma(\gamma_a - \gamma_b)}{[M_f(1-\sigma) + \sigma]^2} \tag{31}$$

$$\sigma = \frac{M_a(\gamma_a-1)}{M_b(\gamma_b-1)} \tag{32}$$

$$\bar{P} = (\gamma-1)\rho e \tag{33}$$

$$P_E = (\gamma-1) \tag{34}$$

$$P_S = e^{\gamma_{M_f}} \tag{35}$$

$$c^2 = \bar{\gamma}\bar{P}/\rho \tag{36}$$

$$\Gamma = \frac{-e^{\gamma_{M_f}}}{(\gamma-1)} \tag{37}$$

where Eqs. (5), (6), and (15) have been used to obtain the last four equations. The specific internal energy is calculated from the conserved variables using Eq. (2).

For a given pair of gases γ_a, γ_b, M_a and M_b are constants along with σ in Eq. (32). Therefore, only Eqs. (30), (31), and (33) through (37) are actually used in the algorithm given in the previous section.

When $\gamma_a = \gamma_b$ and $M_a = M_b$ all of the results reduce to those given in References 1, 6, and 7, and the last of Eqs. (1) for S is not needed. However, as will be shown below, even for a single gas species some useful information can often be obtained by retaining it.

---

[1]Harten, A., "High Resolution Schemes for Hyperbolic Conservation Laws," Journal of Computational Physics, Vol. 49, 1983, pp. 357-393.

[6]Yee, H. C., Warming, R. F., and Harten, A., "A High-Resolution Numerical Technique For Inviscid Gas-Dynamic Problems With Weak Shocks," Preprint for Proceedings of the Eighth International Conference on Numerical Methods in Fluid Dynamics, Aachen, West Germany, June 1982.

[7]Yee, H. C., Warming, R. F., and Harten, A., "Implicit Total Variation Diminishing (TVD) Schemes for Steady-State Calculations," NASA Technical Memorandum 84342, March 1983.

BOUNDARY CONDITIONS

Along the X-axis the symmetry condition was applied in the usual manner by using mirror images of points in the active mesh but with the sign of the v-component of velocity changed. The inflow boundary was handled either by using a known solution, as in the test problem of the next section, or by zeroth-order extrapolation of characteristic variables (refs 9,10) as will be explained below.

For the X-sweep along the vertical wall (see Figure 1), the reflection method was used. For the Y-sweep flow separation was assumed and an extra point was added at the corner - point "b" in the sketch below. The wall boundary condition dictates that $u = 0$. Since there can be no flow across the contact surface, $v = 0$ must apply. Therefore, the same particle remains there

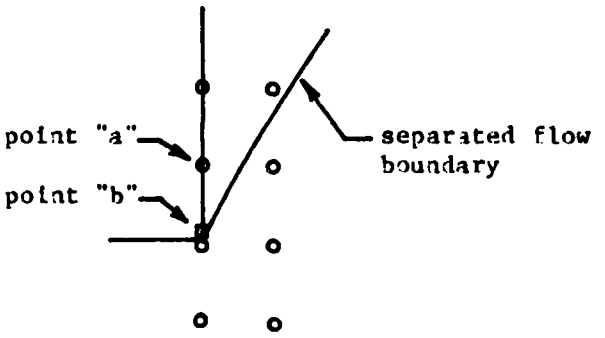

[9]Harten, A., "On a Large Time-Step High Resolution Scheme," ICASE Report No. 82-34, NASA Langley Research Center, Hampton, VA, November 15, 1982.

[10]Yee, H. C., Beam, R. M., and Warming, R. F., "Boundary Approximations for Implicit Schemes for One-Dimensional Inviscid Equations of Gas Dynamics," AIAA Journal, Vol. 20, No. 9, September 1982, pp. 1203-1211.

and its mass fraction remains constant, i.e., $M_f = 1$ if the particles in the environment are identified as species "a". The remaining unknowns are density and energy so two equations are needed. Because v = 0 at the corner, information should reach it from point "a" only through the (v-c) characteristic variable. The characteristic variables for the Y-sweep are $w = L_Y U$ where L_Y is given by Eq. (20). The first characteristic variable corresponding to the (v-c) eigenvalue is

$$w^1 = [(\hat{v}/\hat{c}+\hat{r})\rho - \hat{u}\hat{q}m - (1/\hat{c} + \hat{v}\hat{q})n + \hat{q}E - \hat{\Gamma}\hat{q}S]/2$$

The approximation $w^1_b = w^1_a$ is used at time $\tau + \Delta\tau$ with $\hat{\rho}$, $\hat{c}$, ... evaluated at the average of the two states.

The second characteristic variable corresponding to the (v) eigenvalue is assumed to remain constant. It is given by

$$w^2 = (1-\hat{r})\rho + \hat{u}\hat{q}m + \hat{v}\hat{q}n - \hat{q}E + \hat{\Gamma}\hat{q}S$$

The assumption is that w^2_b at time τ is equal to w^2_b at $\tau + \Delta\tau$. The average state values of $\hat{u}$, $\hat{v}$, and $\hat{\Gamma}$ are always zero.

The procedure is as follows:

1. Apply the operator L_Y to the points along the wall starting with point "a". This requires information at point "b" at time τ, which is available, and information at a second point <u>below</u> "b" because Harten's method is a five-point scheme; it is needed to calculate $g^k_{i,j-1}$ at "b". Since it is not available, $g^k_{i,j}$ at point "a" is used.

2. Solve the two characteristic relations listed above to obtain ρ_b and E_b at time $\tau + \Delta\tau$. Iteration is required because the average state values depend on the new solution at "b".

One final note: It was found through experience that the X-sweep generally could not be applied to the first one or two points along the wall without generating physically unrealistic results there. It will be seen in the next section that this extremely crude handling of the corner flow does not seem to have a drastic impact on the rest of the flow field. This may be true because the inflow boundary condition is so dominant.

A TEST PROBLEM

The classic shock diffraction experiments of Skews (refs 2,3) contain many of the features of the flow sketched in Figure 1 and afford an excellent test problem. Superimposed upon the density contour plot in Figure 2 are Skews' data for a planar shock ($\varepsilon = 0$) with Mach number $M_o = 3$ diffracting around a 90 degree corner. The flow behind the shock is supersonic for this case so the disturbed region lies entirely downstream of the corner. The inflow boundary conditions upstream were constant during the calculation.

The construction of Figure 2 is facilitated by the self-similar nature of the planar flow (ref 11). Thus, the unsteady numerical solution can be compared to the unsteady laboratory experiment at arbitrary times if the data are scaled using the similarity variables

$$\xi = \frac{x'}{c_o t} = \frac{X}{\sqrt{\gamma}\tau} \quad , \quad \eta = \frac{y'}{c_o t} = \frac{Y}{\sqrt{\gamma}\tau}$$

---

[2]Skews, B. W., "The Shape of a Diffracting Shock Wave," Journal of Fluid Mechanics, Vol. 29, Part 2, 1967, pp. 297-304.

[3]Skews, B. W., "The Perturbed Region Behind a Diffracting Shock Wave," Journal of Fluid Mechanics, Vol. 29, Part 4, 1967, pp. 705-719.

[11]Jones, P. M., Martin, P. M. E., and Thornhill, C. K., "A Note on the Pseudo-Stationary Flow Behind a Strong Shock Diffracted or Reflected at a Corner," Proceedings of the Royal Society, A209, 1959, pp. 238-248.

Here c_o is the acoustic speed in the undisturbed environment; for an ideal gas $c_o = \sqrt{\gamma P_o/\rho_o}$. The factor $\sqrt{\gamma}$ appears in the denominator because τ is non-dimensionalized with $\sqrt{P_o/\rho_o}$ in the present study. The numerical data in Figure 2 were obtained after 135 cycles on a uniform grid with 150 cells in the X-direction and 190 cells in the Y-direction; γ was taken as 1.4 for air.

The predicted shock position agrees with Skews' measurements (see Table I) to within three percent everywhere. Note that the inflection point in the experimental data near the wall is also present in the numerical solution. It corresponds to a Mach reflection.

TABLE I. SHOCK POSITION (ESTIMATED FROM FIGURE 3 OF REF 2)

ξ	η
2.75	0.00
2.41	0.65
1.99	1.15
1.48	1.48
0.95	1.65
0.44	1.64
0.00	1.58

The disturbance which propagates downward into the uniform flow behind the shock consists of two segments, the Mach line or leading edge of the Prandtl-Meyer expansion centered at the corner and a circular soundwave. Using expressions given by Skews (ref 2) and the nomenclature of Figure 3

---

[2]Skews, B. W., "The Shape of a Diffracting Shock Wave," Journal of Fluid Mechanics, Vol. 29, Part 2, 1967, pp. 297-304.

the following can be written:

$$\kappa = \frac{c_1 t}{c_o t} = \frac{c_1}{c_o} = \sqrt{1 + \frac{2(\gamma-1)}{(\gamma+1)^2}(M_o^2-1)(\gamma+1/M_o^2)}$$

$$u_p = \frac{u_1}{c_o} = \frac{2}{(\gamma+1)}\left(M_o - \frac{1}{M_o}\right)$$

$$M_1 = \frac{u_1}{c_1} = \frac{u_1}{c_o}\frac{c_o}{c_1} = \frac{u_p}{\kappa}$$

$$\mu = \sin^{-1}(1/M_1)$$

$$\tan^2 \alpha = u_p[(\gamma-1)M_o^2/2 + 1]/M_o^3$$

$$\xi_o = M_o \qquad \eta = -\xi_o \tan \alpha$$

$$\xi_1 = u_p \qquad \eta_1 = -\kappa$$

$$\xi_t = \xi_1 - \kappa \sin \mu \qquad \eta_t = -\kappa \cos \mu$$

where κ is the ratio of acoustic speeds across the shock and u_p is the dimensionless particle velocity behind the shock. Points along the Mach line are computed from

$$\eta = -\xi \tan \mu$$

and intermediate points on the circular arc are given by

$$(\xi-\xi_1)^2 + \eta^2 = \eta_1^2$$

The numerical solution smears the leading edge of the Prandtl-Meyer expansion slightly so that the first contour line does not exactly coincide with the Mach line. The corner approximation may also have influenced the result. Elsewhere the agreement is satisfactory.

The terminator angle, δ, was estimated to be 20 degrees ((ref 3), Figure

---

[3]Skews, B. W., "The Perturbed Region Behind a Diffracting Shock Wave," Journal of Fluid Mechanics, Vol. 29, Part 4, 1967, pp. 705-719.

6). It marks the end of the expansion fan and the beginning of a small region of uniform flow as discussed in Reference 11. The contours in Figure 2 conform to this description.

The slipstream angle, ω, was estimated to be 40 degrees ((ref 3), Figure 5). Skews used it as a reference line along which was measured the intersections of the second (recompression) shock and the contact surface. The contact surface in Figure 2, indicated by the thin solid line following the shock, represents the boundary separating the particles which were processed by the shock before it reached the corner from those processed after it diffracted. It is obtained from the numerical solution by "tagging" one set of particles as "species b" and assigning them a mass function $M_f = 0$. Both sets of particles are given the same molecular weight and specific heat ratio so Γ is zero everywhere. The solution evolves independently of the species equation. The contact surface, initially a vertical line at $\xi = 0$, is simply convected downstream by the velocity field. Note that it passes through the low point ξ_1, η_1 of the soundwave. This is correct because all of the particles below the soundwave move at the particle velocity behind the shock, $u_p = \xi_1$.

The intersection of the contact surface with the slipstream angle, indicated by the asterisk in Figure 2, was estimated to be 1.65 ((ref 3), Figure 8c). Its coordinates ξ_c, η_c are

---

[3]Skews, B. W., "The Perturbed Region Behind a Diffracting Shock Wave," Journal of Fluid Mechanics, Vol. 29, Part 4, 1967, pp. 705-719.

[11]Jones, P. M., Martin, P. M. E., and Thornhill, C. K., "A Note on the Pseudo-Stationary Flow Behind a Strong Shock Diffracted or Reflected at a Corner," Proceedings of the Royal Society, A209, 1959, pp. 238-248.

$$\xi_c = 1.65 \cos 40° = 1.264$$

$$\eta_c = 1.65 \sin 40° = 1.061$$

The numerical solution comes very close to passing through this point.

It should be noted that the contact surface described above and that discernible in a shadowgraph are not the same. The contact surface discussed by Skews actually represents the boundary separating those particles which were processed by the planar shock from those processed by the diffracted shock. It is associated with the entropy gradient along the curved portion of the shock and can be identified in Figure 4 as the entropy contour which intersects the point where the shock ceases to be planar. This contour coincides with the "kink" in each of the density contours in Figure 2 which renders it visible on a shadowgraph. At the point where Skews' measurement was taken the entropy contour and the contact surface nearly conicide which accounts for the agreement noted above.

The second shock location, indicated by the star in Figure 3, was estimated to be 1.2 ((ref 3), Figure 7c). Its coordinates ξ_s, η_s are

$$\xi_s = 1.2 \cos 40° = 0.919$$

$$\eta_s = 1.2 \sin 40° = 0.717$$

Again, the numerical solution does fairly well.

The vortex angle, ψ, and its location indicated by the diamond in Figure 2, were estimated to be 48 degrees and 1.15, respectively ((ref 3), Figure 9). Its coordinates, ξ_v, η_v are

---

[3]Skews, B. W., "The Perturbed Region Behind a Diffracting Shock Wave," Journal of Fluid Mechanics, Vol. 29, Part 4, 1967, pp. 705-719.

$$\xi_v = 1.15 \cos 48° = 0.669$$

$$\eta_v = 1.15 \sin 48° = 0.743$$

Judging by the density contours, the proper vortex angle seems to have been computed but its position appears somewhat closer to the corner than measured by Skews. However, identifying the vortex center from a shadowgraph involves a greater degree of uncertainty than the other measurements so the apparent discrepancy may not be serious.

CONCLUSION

The test problem of the last section demonstrates that Harten's TVD method can be used to obtain reasonably accurate solutions for the flow problems of interest. In a companion report (ref 4), the method is applied to a problem involving two gases.

---

[4]Carofano, G. C., "Secondary Waves From Nozzle Blast," U.S. ARDC Technical Report No. ARLCB-TR-84028, Benet Weapons Laboratory, Watervliet, NY, October 1984.

REFERENCES

1. Harten, A., "High Resolution Schemes for Hyperbolic Conservation Laws," Journal of Computational Physics, Vol. 49, 1983, pp. 357-393.
2. Skews, B. W., "The Shape of a Diffracting Shock Wave," Journal of Fluid Mechanics, Vol. 29, Part 2, 1967, pp. 297-304.
3. Skews, B. W., "The Perturbed Region Behind a Diffracting Shock Wave," Journal of Fluid Mechanics, Vol. 29, Part 4, 1967, pp. 705-719.
4. Carofano, G. C., "Secondary Waves From Nozzle Blast," U.S. ARDC Technical Report No. ARLCB-TR-84028, Benet Weapons Laboratory, Watervliet, NY, October 1984.
5. Obert, E. F., Concepts of Thermodynamics, McGraw-Hill Book Co. Inc., New York 1960, Equation 11-1b.
6. Yee, H. C., Warming, R. F., and Harten, A., "A High-Resolution Numerical Technique for Inviscid Gas-Dynamic Problems With Weak Shocks," Preprint for Proceedings of the Eighth International Conference on Numerical Methods in Fluid Dynamics, Aachen, West Germany, June 1982.
7. Yee, H. C., Warming, R. F., and Harten, A., "Implicit Total Variation Diminishing (TVD) Schemes for Steady-State Calculations," NASA Technical Memorandum 84342, March 1983.
8. Obert, E. F., Concepts of Thermodynamics, McGraw-Hill Book Co. Inc., New York, 1960, Chapter 8.
9. Harten, A., "On a Large Time-Step High Resolution Scheme," ICASE Report No. 82-34, NASA Langley Research Center, Hampton, VA, November 15, 1982.

10. Yee, H. C., Beam, R. M., and Warming, R. F., "Boundary Approximations for Implicit Schemes for One-Dimensional Inviscid Equations of Gas Dynamics," AIAA Journal, Vol. 20, No. 9, September 1982, pp. 1203-1211.

11. Jones, P. M., Martin, P. M. E., and Thornhill, C. K., "A Note on the Pseudo-Stationary Flow Behind a Strong Shock Diffracted or Reflected at a Corner," Proceedings of the Royal Society, A209, 1959, pp. 238-248.

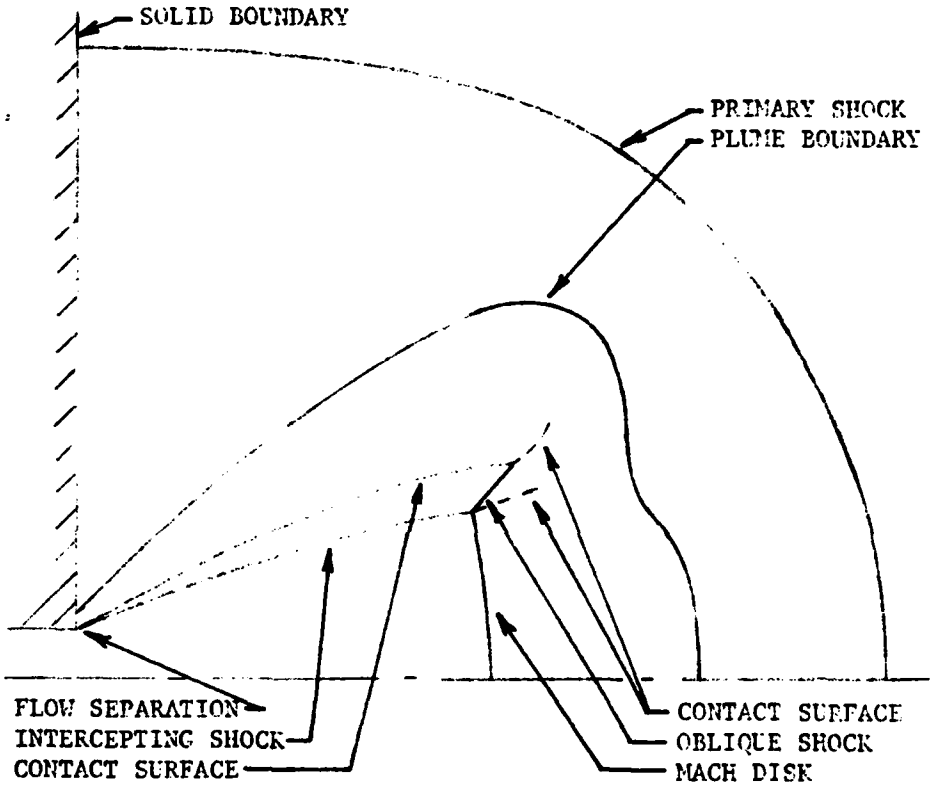

Figure 1. Typical Flow Field Structure.

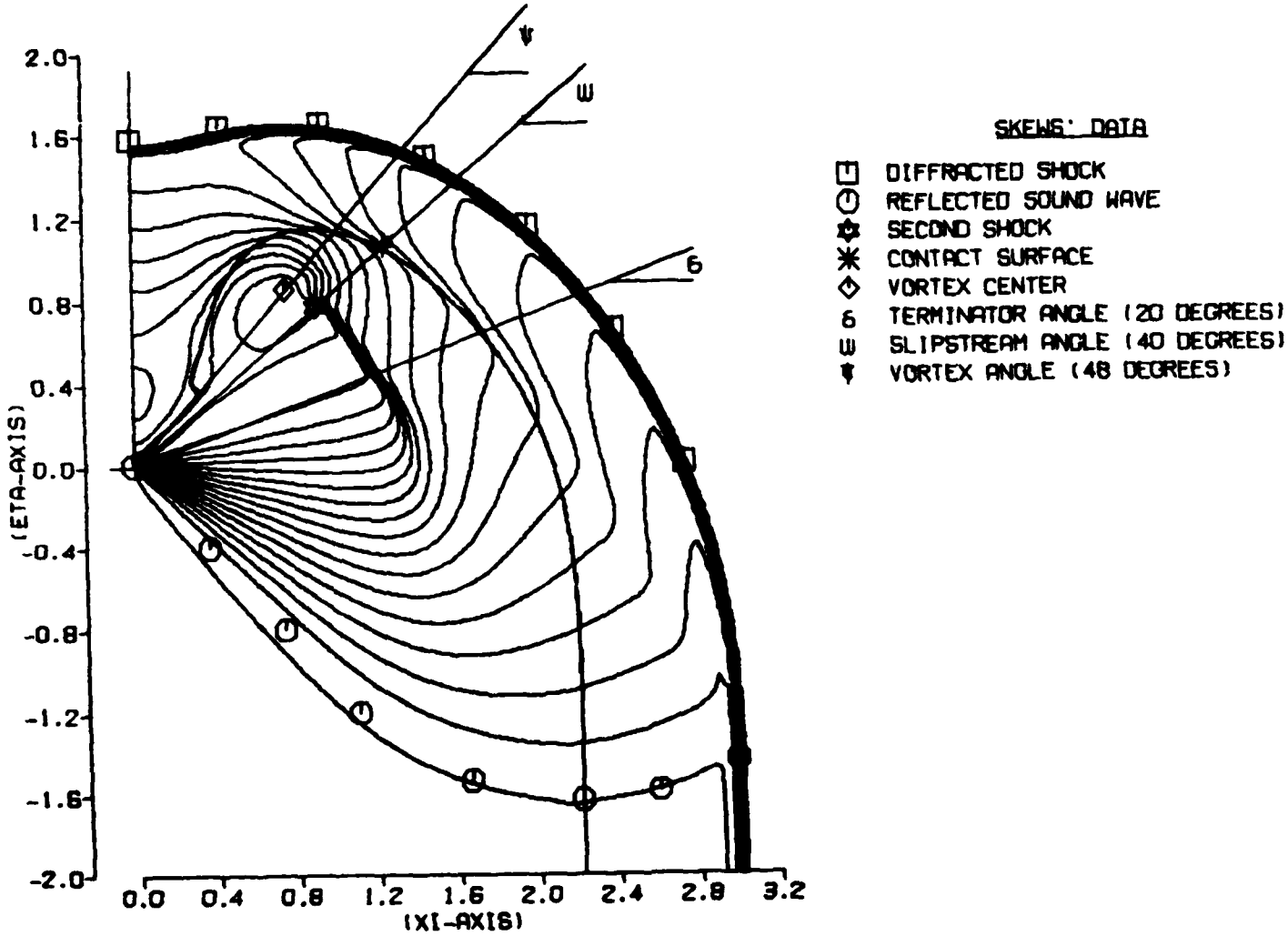

Figure 2. Comparison of Skews' Data with Density Contour Plot.

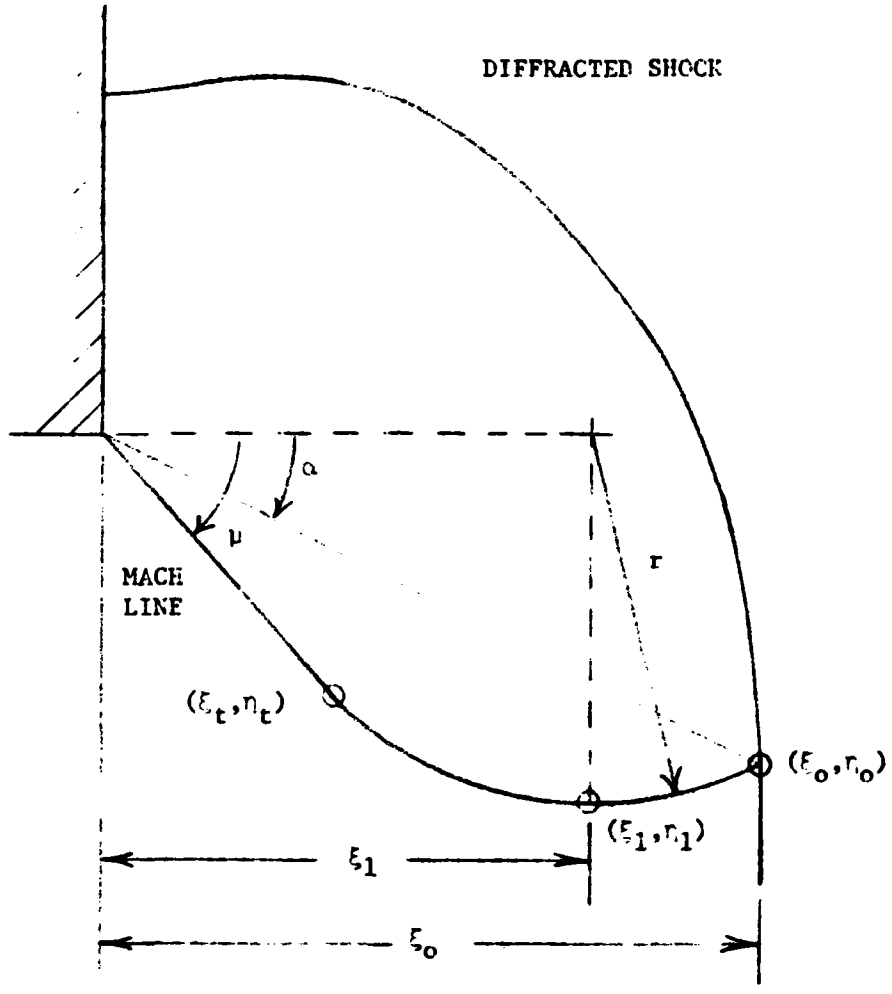

Figure 3. Reflected Soundwave Nomenclature.

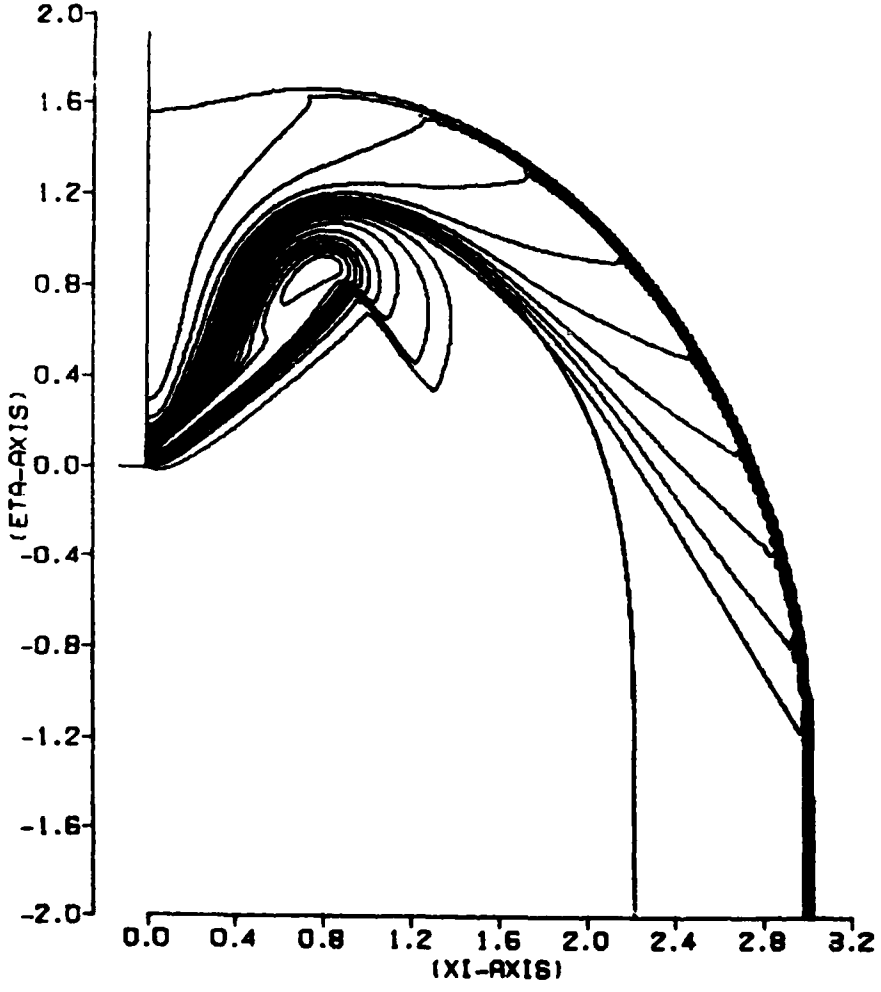

Figure 4. Entropy Contour Plot.

TECHNICAL REPORT INTERNAL DISTRIBUTION LIST

	NO. OF COPIES
CHIEF, DEVELOPMENT ENGINEERING BRANCH	
ATTN: SMCAR-LCB-D	1
-DA	1
-DP	1
-DR	1
-DS (SYSTEMS)	1
-DS (ICAS GROUP)	1
-DC	1
CHIEF, ENGINEERING SUPPORT BRANCH	
ATTN: SMCAR-LCB-S	1
-SE	1
CHIEF, RESEARCH BRANCH	
ATTN: SMCAR-LCB-R	2
-R (ELLEN FOGARTY)	1
-RA	1
-RM	2
-RP	1
-RT	1
TECHNICAL LIBRARY ATTN: SMCAR-LCB-TL	5
TECHNICAL PUBLICATIONS & EDITING UNIT ATTN: SMCAR-LCB-TL	2
DIRECTOR, OPERATIONS DIRECTORATE	1
DIRECTOR, PROCUREMENT DIRECTORATE	1
DIRECTOR, PRODUCT ASSURANCE DIRECTORATE	1

NOTE: PLEASE NOTIFY DIRECTOR, BENET WEAPONS LABORATORY, ATTN: SMCAR-LCB-TL, OF ANY ADDRESS CHANGES.

TECHNICAL REPORT EXTERNAL DISTRIBUTION LIST

	NO. OF COPIES
ASST SEC OF THE ARMY RESEARCH & DEVELOPMENT ATTN: DEP FOR SCI & TECH THE PENTAGON WASHINGTON, D.C. 20315	1
COMMANDER DEFENSE TECHNICAL INFO CENTER ATTN: DTIC-DDA CAMERON STATION ALEXANDRIA, VA 22314	12
COMMANDER US ARMY MAT DEV & READ COMD ATTN: DRCDE-SG 5001 EISENHOWER AVE ALEXANDRIA, VA 22333	1
COMMANDER ARMAMENT RES & DEV CTR US ARMY AMCCOM ATTN: SMCAR-LC	1
SMCAR-LCE	1
SMCAR-LCM (BLDG 321)	1
SMCAR-LCS	1
SMCAR-LCU	1
SMCAR-LCW	1
SMCAR-SCM-O (PLASTICS TECH EVAL CTR, BLDG. 351N)	1
SMCAR-TSS (STINFO) DOVER, NJ 07801	2
DIRECTOR BALLISTICS RESEARCH LABORATORY ATTN: AMXBR-TSB-S (STINFO) ABERDEEN PROVING GROUND, MD 21005	1
MATERIEL SYSTEMS ANALYSIS ACTV ATTN: DRXSY-MP ABERDEEN PROVING GROUND, MD 21005	1
COMMANDER US ARMY AMCCOM ATTN: SMCAR-ESP-L ROCK ISLAND, IL 61299	1
COMMANDER ROCK ISLAND ARSENAL ATTN: SMCRI-ENM (MAT SCI DIV) ROCK ISLAND, IL 61299	1
DIRECTOR US ARMY INDUSTRIAL BASE ENG ACTV ATTN: DRXIB-M ROCK ISLAND, IL 61299	1
COMMANDER US ARMY TANK-AUTMV R&D COMD ATTN: TECH LIB - DRSTA-TSL WARREN, MI 48090	1
COMMANDER US ARMY TANK-AUTMV COMD ATTN: DRSTA-RC WARREN, MI 48090	1
COMMANDER US MILITARY ACADEMY ATTN: CHMN, MECH ENGR DEPT WEST POINT, NY 10996	1
US ARMY MISSILE COMD REDSTONE SCIENTIFIC INFO CTR ATTN: DOCUMENTS SECT, BLDG. 4484 REDSTONE ARSENAL, AL 35898	2
COMMANDER US ARMY FGN SCIENCE & TECH CTR ATTN: DRXST-SD 220 7TH STREET, N.E. CHARLOTTESVILLE, VA 22901	1

NOTE: PLEASE NOTIFY COMMANDER, ARMAMENT RESEARCH AND DEVELOPMENT CENTER, US ARMY AMCCOM, ATTN: BENET WEAPONS LABORATORY, SMCAR-LCB-TL, WATERVLIET, NY 12189, OF ANY ADDRESS CHANGES.

TECHNICAL REPORT EXTERNAL DISTRIBUTION LIST (CONT'D)

	NO. OF COPIES
COMMANDER US ARMY MATERIALS & MECHANICS RESEARCH CENTER ATTN: TECH LIB - DRXMR-PL WATERTOWN, MA 01272	2
COMMANDER US ARMY RESEARCH OFFICE ATTN: CHIEF, IPO P.O. BOX 12211 RESEARCH TRIANGLE PARK, NC 27709	1
COMMANDER US ARMY HARRY DIAMOND LAB ATTN: TECH LIB 2800 POWDER MILL ROAD ADELPHIA, MD 20783	1
COMMANDER NAVAL SURFACE WEAPONS CTR ATTN: TECHNICAL LIBRARY CODE X212 DAHLGREN, VA 22448	1

	NO. OF COPIES
DIRECTOR US NAVAL RESEARCH LAB ATTN: DIR, MECH DIV CODE 26-27, (DOC LIB) WASHINGTON, D.C. 20375	1 1
COMMANDER AIR FORCE ARMAMENT LABORATORY ATTN: AFATL/DLJ AFATL/DLJG EGLIN AFB, FL 32542	1 1
METALS & CERAMICS INFO CTR BATTELLE COLUMBUS LAB 505 KING AVENUE COLUMBUS, OH 43201	1

NOTE: PLEASE NOTIFY COMMANDER, ARMAMENT RESEARCH AND DEVELOPMENT CENTER, US ARMY AMCCOM, ATTN: BENET WEAPONS LABORATORY, SMCAR-LCB-TL, WATERVLIET, NY 12189, OF ANY ADDRESS CHANGES.